Health and Technology (2020) 10:385–390
https://doi.org/10.1007/s12553-019-00355-y

ORIGINAL PAPER

Check for updates

Mapping the friction coefficient of AISI 316L on UHMWPE lubricated with bovine serum to study the effect of loading and entrainment at high values of sliding-to-rolling ratio

J. L. Montes-Seguedo[1] · A. L. Garcia-Garcia[1] · J. D. O. Barceinas-Sanchez[1] · J. C. Sosa-Savedra[1] · M. R. J. Morales-Garcia[1] · E. Gonzalez-Jasso[1] · I. Dominguez-Lopez[1]

Received: 18 January 2019 / Accepted: 2 August 2019 / Published online: 9 August 2019
© IUPESM and Springer-Verlag GmbH Germany, part of Springer Nature 2019

Abstract

From an experimental point of view, determining the lubrication regime established between contact surfaces of joint prosthesis using the theory of elastohydrodynamic lubrication is rather impractical due to the intrinsic hindrances to measure the thickness of the lubricant film at the contact area. This claim is supported by the results obtained by experts using optical interferometry to perform such measurements using synovial like fluids. Similarly, research has shown that the complex rheology of the synovial fluid complicates the direct application of EHL theory and plays an important role in the lubrication mechanisms at work in prosthetic devices. Since the natural response of all tribological systems is the frictional force, rather than trying to measure the thickness of the lubricant film to determine the lubrication regime, we measured the effect of loading and entrainment on the friction coefficient at the contact point of an AISI 316L stainless steel sphere loaded against an ultra-high molecular weight polyethylene disc, lubricated with fetal bovine serum solution, at high values of sliding-to-rolling ratio. Applying statistical analysis, we obtained a best-fit model that shows a smooth transition from mixed to full-film lubrication regime

Keywords AISI 316L/UHMWPE · Fetal bovine serum · Friction coefficient · Protein assisted lubrication

1 Introduction

Natural joint lubrication has been subject to study since the 1960s [1–3]. To understand the lubrication mechanisms at work in total joint replacements, numerical and experimental approaches have been undertaken to relate the behavior of the friction coefficient (COF) and wear with lubricant film-thickness [1, 4–7]. The COF between two rubbing surfaces in dry contact is defined as the ratio of lateral friction force to normal load. When a lubricant is introduced, the dragging forces associated with the shearing stresses within the fluid moving between the counterparts must be considered. Most mathematical models for lubrication rely on the definition of suitable, simplified viscosity functions to mimic the non-Newtonian nature of synovial fluids, without fully grasping their complex rheological behavior [8].

A number of theoretical and experimental studies of lubrication regimes have focused on the COF between different tribopairs, using either synthetic or biological fluids [9–14]. For instance, under some experimental conditions, mixed lubrication was reported for CoCrMo on ultra-high molecular weight polyethylene (UHMWPE), lubricated with fetal bovine serum (FBS) [15, 16]. On the other hand, Murakami and Otsuki [17] reported using silicon oil to study the behavior of the lubricant film between the surfaces of a specific model of total knee replacement (TKR). Their results showed a clear dependence between the thickness of the lubricant film and the phase of a non-standardized walking cycle.

Other researchers have applied the theory of elastohydrodynamic lubrication (EHL), both numerically and experimentally, to predict the behavior of the lubrication mechanisms in joint-related tribopairs [18–21]. To this respect, Hook and Huang [22] demonstrated that, for a line contact, the viscoelastic properties of the soft material in the

✉ I. Dominguez-Lopez
idominguezl@ipn.mx

1 Instituto Politecnico Nacional, Centro de Investigacion en Ciencia Aplicada y Tecnologia Avanzada, Unidad Queretaro, Cerro Blanco No.141, 76090 Queretaro, Qro., Mexico

tribopair might play an important role in the lubrication process. From the experimental side, lubrication regimes in hip joint replacements have been amply investigated using optical interferometry [23]. The main conclusion of this line of research is that protein rheology, complicated by protein-protein and protein-surface interactions, renders the EHL theory useless to explain the thickness of the observed films. The tribopairs were not the ones used in real-life devices and, due to the restrictions of the experimental technique, the loading and kinematics at the contact point reproduced only a few clinically significant values of the corresponding walking cycle.

Experimental intervals for the independent variables were established for the present work from previously observed behavior of the COF during the walking cycle, reported by Barceinas et al. [24] for a specific commercial model of knee prosthesis were the loading pressure (P_m), entrainment speed (V_m), and sliding-to-rolling ratio (SRR) were obtained from the loading cycle and arthrokinematics prescribed by the ISO 14243-3:2014 standard [25]. Due to the constant variations of the parameters along the walking cycle, which is generally divided into stance and swing phases [26], the lubrication regime of the tribosystem gets masked. During the swing phase, we found that SRR is larger than 2 for the most part, peaking at about 20 [24]. Under this condition, both surfaces of the tribopair move in opposite directions. For clarity and simplicity purposes, we designate the kinematics for which SRR>3 as super-sliding.

To improve our understanding of protein assisted lubrication (PAL) during the rubbing of AISI 316L on UHMWPE under super-sliding conditions when lubricated with FBS solutions at 37 °C, we performed a systematic study of the behavior of the COF within the chosen experimental intervals. Presumably, under these experimental conditions, protein interactions should have less of an effect on lubrication, leading to EHL as the expected lubrication regime for the tribosystem.

2 Materials and methods

2.1 Experimental setup

Figure 1 depicts a schematic representation of the experimental apparatus, described by Barceinas et al. [24]. In this experimental setup, an AISI 316L stainless steel ball (diameter: 19.05 mm, maximum surface roughness of 0.127 μm), is loaded against the face of an UHMWPE disc, backed with an AISI 316L stainless steel disc. The instrument only takes integer values for load L, in newton. The lubricant cup possesses a temperature control graded in Celsius.

The ball-on-disc tribometer measures the COF as a function of $SRR = |V_r/V_m|$, where the relative and entrainment speeds at the contact point are defined as $|V_r| = |V_1 - V_2|$ and $|V_m| = |(V_1 + V_2)/2|$, respectively. Both the ball and the disc rotate independently from one another, thus creating a variety of kinematic conditions: rolling without sliding (SRR = 0), rolling while sliding (0 < SRR < 2), sliding (SRR = 2), and super-sliding (SRR > 2).

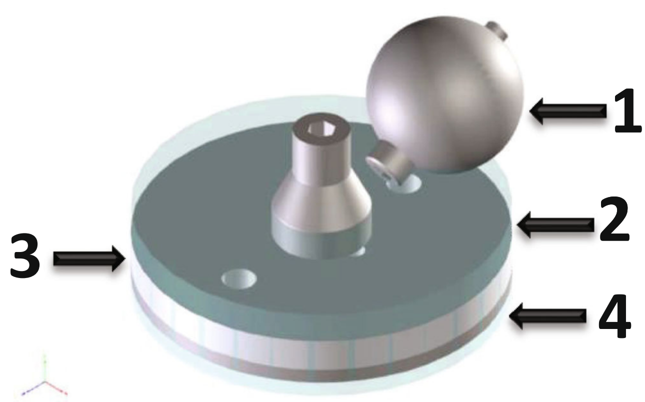

Fig. 1 Schematic representation of ball-on-disc tribometer. (1) AISI 316L ball, (2) Lubricant, (3) UHMWPE disc, and (4) AISI 316L support

The input variables in the MTM2 tribometer from PCS Instruments (London, UK) include the sliding-to-rolling ratio (SRR), the entrainment speed (V_m), the load (L), and the temperature (T) of the lubricant fluid.

2.2 Surface preparation

We obtained a number of slices from an as received UHMWPE white bar (diameter: 50.8 mm); these were rectified to a thickness of 4.20 ± 0.03 mm, then lathed down to a diameter of 46 mm. After the machining process, the discs were wet ground in running water until obtaining a center-line average roughness R_a= 0.025 ± 0.016 μm,

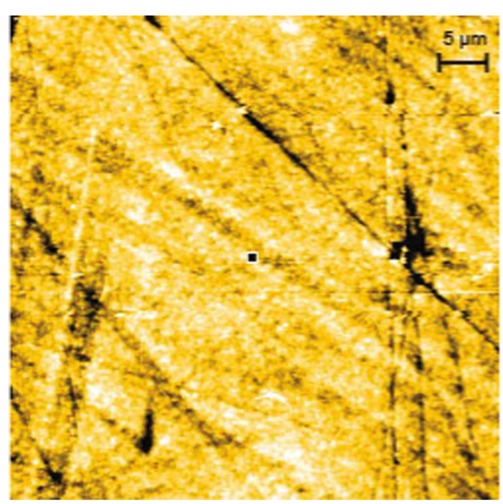

Fig. 2 Surface topography of the polished UHMWPE surface measured by AFM

Table 1 Experimental design with three factors

Independent variables		
P_m (MPa)	SRR	$\lvert V_m \rvert$ (mm/s)
19.1, 24.1, 27.6	3 – 21 steps of 2	10 – 100 steps of 10

as measured with an atomic force microscope EasyScan2 from Nanosurf (Liestal, Switzerland). In Fig. 2, we shows a typical AFM image of the sample surface.

2.3 Lubricant fluid

As for the lubricant testing fluid, we diluted as received bovine serum S1650 FBS (Biowest SAS, Nuaillé, France) with deionized and sterilized water until achieving a protein mass concentration of 20 g/L. Although the ISO standard makes allowances for the use of anti-microbial reagents, we dispensed with their use for the present work. To avoid sample contamination, we sterilized the laboratory materials for 15 minutes at 125 °C at 0.15 MPa in a LS-B7SL autoclave from Labtronic. The dilution was performed under an AHC-40 laminar flow hood from Esco.

2.4 Experimental design

Table 1 summarizes the experimental design that we used. We obtained the contact pressure values (P_m) from Hertz contact theory considerations [24], corresponding to loads of 3, 6, and 9 N. The SRR values range from 3 to 21 in steps of 2, whereas $|V_m|$ increased from 10 to 100 mm/s in steps of 10 mm/s.

We used a disc for each level of load, measuring the COF for all possible combinations of SRR and V_m, within their respective range intervals. Since all three levels of load were randomized, each complete repetition of the experiment required three discs.

3 Results and analysis

We measured the COF five times along the entire V_m range, for each combination of the (P_m, SRR, V_m) triads. We depict typical results of these measurements in Fig. 3 for SRR values of 3, 7, 11, and 21, and for load L = 3 N, equivalent to a contact pressure of 19.1 MPa.

3.1 Regression analysis

We developed the prediction model using Design Expert™, adopting as significance level α = 0.05. The simplest best-

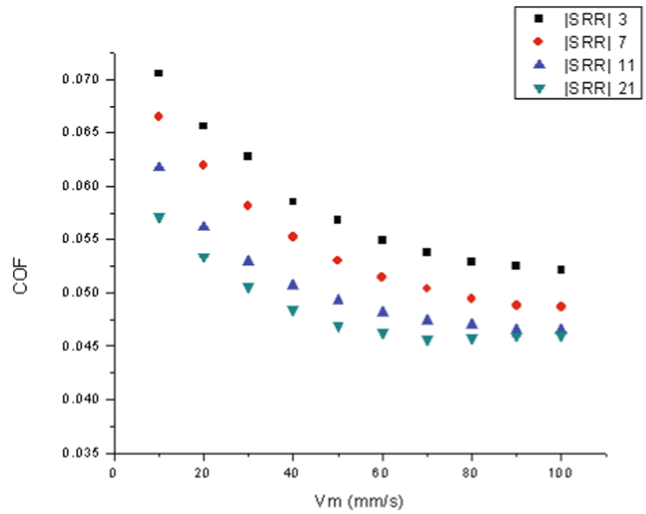

Fig. 3 Typical Stribeck curves for the maximum contact pressure Pm = 19.1 MPa

fit model obtained for the experimental data was the power law model in Eq. 1:

$$COF = b_0 \cdot P_m^{b_1} \cdot SRR^{b_2} \cdot |V_m|^{b_3} \quad (1)$$

with determination coefficient R^2 = 0.95. The corresponding ANOVA results showed that P_m, SRR, and $|V_m|$ had significant effects on the COF. The power law model in Eq. 1 explains 95% of the variability in the COF. All the three factors related inversely to it; however, the effect of P_m was almost six-fold larger than either SRR or $|V_m|$, as can be observed in Table 2. The details on the regression analysis can be consulted in Appendix A.

In Fig. 3, we can observe that the COF is a monotonic decreasing function of $|V_m|$, rather than following the more complicated variations of the COF reported by Lopez et al. [27] for water, which is a Newtonian fluid.

We obtained the response surfaces of the regression model in Eq.1 for all three levels of contact pressure, then contrasted them with the experimental data. As we show in Fig. 4, the regression model fits fairly well with the experimental data. The highest values of COF are observed at the lowest end of SRR and $|V_m|$.

For the lowest level of contact pressure (see Fig. 4a) the experimental data are distributed above and below the response surface; however, for the 24.1 MPa contact pressure (see Fig. 4b) the model overestimates the experimental COF in

Table 2 Power law model for the COF

	$COF = b_0 P_m^{b_1}\ SRR^{b_2} \lvert V_m \rvert^{b_3}$				
	b_0	b_1	b_2	b_3	R^2
COF (@ 20 g/L)	0.54	-0.58	-0.10	-0.10	0.95

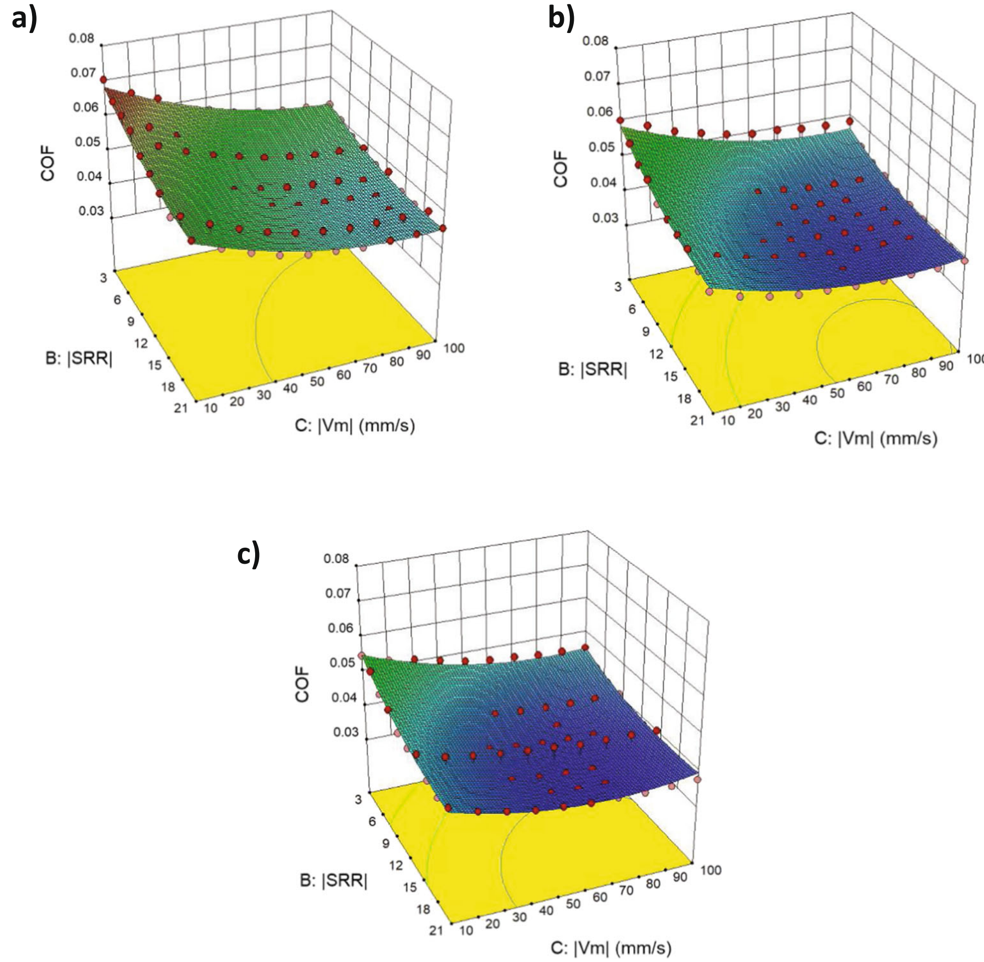

Fig. 4 Response surface of the models of powers. **a** P_m = 19.1 MPa, **b** P_m = 24.1 MPa, and **c** P_m = 27.6 MPa

almost the entire surface, except for SRR = 3, where the highest value of COF is observed at the lowest value of $|V_m|$. For the highest level of contact pressure (see Fig. 4c) the experimental data are fairly evenly distributed above and below the response surface, overestimating at low values of SRR and entrainment. In the three cases, the COF is highest at the low ends of the experimental conditions, i.e. low SRR and $|V_m|$. Under these conditions, the relative speed between the surfaces is 30 mm/s, which is small enough for the proteins to interact with each other, thus contributing to increase the COF [28].

4 Conclusions

The power law expression developed herein explains 95% of the experimental results obtained for the response variable, and it is consistent with regression models obtained for the more complicated variations of the experimental parameters during a stride [8, 24]. Using different types of lubricant fluids, de Vicente et al. [29] developed regression models for Newtonian fluids which also involved powers of SRR, entrainment, and load. In their research, the dependence between the COF and the SRR is direct, rather than inverse. Garcia et al. [8] reported similar results for water under the kinematics and loading conditions of the walking cycle, while Lopez et al. [27] did it under experimental conditions similar to the ones in the present work. We conclude, therefore, that the inverse relation observed between the COF and SRR is due to the presence of proteins in the lubricant fluid. At high values of SRR, a smooth transition from mixed to full-film lubrication occurs, as $|V_m|$ and SRR increase.

Acknowledgments The authors gratefully acknowledge financial support from Instituto Politecnico Nacional and CONACYT to carry on the present work, via grants SIP20180863 and PDCPN 2014-248639, respectively. Financial support to carry on graduate studies has also been provided by CONACYT and is gratefully acknowledged (JLMS).

Funding This study was funded by Instituto Politecnico Nacional (SIP20180863) and CONACYT (PDCPN 2014-248639).

Compliance with Ethical Standards

Conflict of interests The authors declare that they have no conflict of interest.

Ethical approval This article does not contain any studies with human participants or animals performed by any of the authors.

Informed consent Informed consent was obtained from all individual participants included in the study.

Appendix A

Results of the ANOVA test on the COF

Full model	COF (@ 20 g/L)				
Source of variation	Sum of squares	Degrees of freedom	Mean square	F value	P value Prob>F
Model	0.94	3	0.31	2022.72	< 0.001
A-Log (pressure)	0.44	1	0.44	2815.16	< 0.001
B-Log (|SRR|)	0.22	1	0.22	1405.43	< 0.001
C-Log ($\|V_m\|$)	0.29	1	0.29	1847.56	< 0.001
Residual	0.046	19	1.56E-4		
R-squared	0.95				
Adj. R-squared	0.95				

References

1. Higginson GR. Elastohydrodynamic lubrication in human joints proceedings of the institution of mechanical engineers. Proceedings of the institution of mechanical engineers. 1977.
2. Dowson D. Paper 12: Modes of lubrication in human joints. Proceedings of the Institution of Mechanical Engineers, Conference Proceedings. 1966.
3. Unsworth A. Tribology of human and artifical joints. Proc Inst Mech Eng H. 1991.
4. Fan J, Myant C, Underwood R, Cann P. Synovial fluid lubrication of artificial joints: protein film formation and composition. The Royal Society of Chemistry. 2012.
5. Björling M, Habchi W, Bair S, Larsson R, Marklund P. Towards the true prediction of EHL friction. Tribol Int. 2013.
6. Habchi W, Bair S, Vergne P. On friction regimes in quantitative elastohydrodynamics. Tribol Int. 2013.
7. Zhang X, Li Z, Wang J. Friction prediction of rolling-sliding contact in mixed EHL. Measurement. 2017.
8. Garcia-Garcia AL, Alvarez-Vera M, Montoya-Santiyanes LA, Dominguez-Lopez I, Montes-Seguedo JL, Sosa-Savedra JC, et al. Regression models to predict the behavior of the coefficient of friction of AISI 316L on UHMWPE under ISO 14243-3 conditions. J Mech Behav Biomed Mater. 2018.
9. Unsworth A, Dowson D, Wright V. Some new evidence on human joint lubrication. Ann Rheum Dis. 1975.
10. Unsworth A, Dowson D, Wright V. The frictional behavior of human synovial joints-part 1: natural joints. J Lubr Technol. 1975.
11. Scholes SC, Unsworth A. Comparison of friction and lubrication of different hip prostheses. Proc Inst Mech Eng H J Eng Med. 2000.
12. Caravia L, Dowson D, Fisher J, Corkhill PH, Tighe BJ. Friction and mixed lubrication in soft layer contacts. In: Dowson D, editor. Thin films in tribology. vol. 25. Elsevier; 1993. p. 529–534.
13. Unsworth A. The effects of lubrication in hip prostheses. Phys Med Biol. 1978.
14. Scholes SC, Unsworth A. The effects of proteins on the friction and lubrication of artificial joints. Proc Inst Mech Eng H J Eng Med. 2006.
15. Scholes SC, Unsworth A. The tribology of metal-on-metal total hip replacements. Proc Inst Mech Eng H J Eng Med. 2006.
16. Hall R, Unsworth A. Friction in hip prostheses. Biomaterials. 1997.
17. Murakami T, Ohtsuki N. Paper XII(iii) Lubricating film formation in knee prostheses under walking conditions. In: Dowson D, Taylor CM, Godet M, Berthe D, editors. Tribology Series. vol. 11. Elsevier; 1987. p. 387–392.
18. Jin ZM, Dowson D, Fisher J, Ohtsuki N, Murakami T, Higaki H, et al. Prediction of transient lubricating film thickness in knee prostheses with compliant layers. Proc Inst Mech Eng H J Eng Med. 1998.
19. Jin ZM, Dowson D. Elastohydrodynamic lubrication in biological systems. Proceedings of the Institution of Mechanical Engineers, Part J: Journal of Engineering Tribology. 2005.
20. Jalali-Vahid D, Jagatia M, Jin ZM, Dowson D. Prediction of lubricating film thickness in UHMWPE hip joint replacements. J Biomech. 2001.
21. Mongkolwongrojn M, Wongseedakaew K, Kennedy FE. Transient elastohydrodynamic lubrication in artificial knee joint with non-Newtonian fluids. Tribol Int. 2010.
22. Hooke CJ, Huang P. Elastohydrodynamic lubrication of soft viscoelastic materials in line contact. Proceedings of the Institution of Mechanical Engineers, Part J: Journal of Engineering Tribology. 1997.
23. Myant CW, Cann P. The effect of transient conditions on synovial fluid protein aggregation lubrication. J Mech Behav Biomed Mater. 2014.
24. Barceinas-Sanchez JDO, Alvarez-Vera M, Montoya-Santiyanes LA, Dominguez-Lopez I, Garcia-Garcia AL. The coefficient of

friction of UHMWPE along an entire walking cycle using a ball-on-disc tribometer under arthrokinematics and loading conditions prescribed by ISO 14243-3:2014. J Mech Behav Biomed Mater. 2017.
25. ISO. ISO 14243-3 (en) Implants for surgery - Wear of total knee-joint prostheses- Part 3: Loading and displacement parameters for wear-testing machines with displacement control and corresponding environmental conditions for test. Int Organ. 2014.
26. Uustal H, Baerga E. Prosthetics and orthotics gait analysis. In: Cuccurullo SJ, editor. Physical Medicine and Rehabilitation Board Review. Third edit ed. Demos Medical Publishing; 2015. p. 409–488.
27. López-Cervantes A, Domínguez-López I, Barceinas-Sánchez JDO, García-García AL. Effects of surface texturing on the performance of biocompatible UHMWPE as a bearing material during in vitro lubricated sliding/rolling motion. J Mech Behav Biomed Mater. 2013.
28. Myant C, Cann P. Review Article On the matter of synovial fluid lubrication: Implications for metal-on-metal hip tribology. J Mech Behav Biomed Mater. 2014.
29. de Vicente J, Stokes JR, Spikes HA. The Frictional properties of Newtonian fluids in rolling–sliding soft-EHL Contact. Tribol Lett. 2005.

Publisher's note Springer Nature remains neutral with regard to jurisdictional claims in published maps and institutional affiliations.